Regular Article

PHYSICAL CHEMISTRY RESEARCH
Published by the
Iranian Chemical Society
www.physchemres.org
info@physchemres.org

***Phys. Chem. Res.**, Vol. 6, No. 1, 173-192, March 2018*
DOI: 10.22036/pcr.2017.82484.1369

Toward the Development of a Robust Kinetic Model for the Cobalt Fischer-Tropsch Catalyst Lifetime Using a Novel Sigmoidal Pattern

M. Khorashadizadeh and H. Atashi*

Department of Chemical Engineering, University of Sistan and Baluchestan, Zahedan, Iran

(Received 16 April 2017, Accepted 23 October 2017)

Catalyst deactivation rate greatly depends on many factors including the catalyst structure, reactor feed composition, and operating conditions. Since catalyst deactivation modeling has so far been poorly addressed in the literature, nine experimental sets of cobalt based Fischer-Tropsch catalysts activity-time data were considered to be modeled using an innovative sigmoidal pattern with amazingly meaningful parameters. Such theoretical models for catalyst lifetime significantly facilitate the control of reactors during petrochemical industrial applications, where a constant reactor product flow rate is necessary. Four types of statistics were used to verify the validity of the regression model. The results showed that the proposed model perfectly predicts the activity of the whole catalyst lifetime for a wide range of catalyst types which is capable of being utilized as an important part of a reaction rate. For process conditions within the range of T = 220-230 °C, P = 20 bar, and H_2/CO ratio = 2, the average of the two important model constants were: 0.6 ± 0.1 and 0.42 ± 0.06 for steady-state activity and total activity loss, respectively. The proposed model offers a significant advance over the existing macroscopic deactivation models, since different catalyst deactivation trends can be captured.

Keywords: CO hydrogenation, Cobalt catalyst, Deactivation modeling, Sigmoidal fit, Thermodynamic equilibrium

INTRODUCTION

Liquid hydrocarbon fuels and several other chemical products can be formed from syngas (CO and H_2) through the famous and recognized catalytic process named Fischer-Tropsch (FT) synthesis (FTS). The syngas can be produced from coal, biomass, and natural gas. Converting natural gas into the liquid products *via* the FTS is enormously of great importance for countries possessing huge natural gas reserves. Moreover, up to date, due to demands for high-quality and environmentally friendly transportation fuels, FTS has been widely explored as a catalytic ultra-clean fuel production approach [1-8].

Among several FT catalysts, only iron and cobalt have found commercial applications. After 9-12 months of operation, expensive cobalt catalyst deactivates, and loses its activity up to 30-50% and suffers from a similar drop in their hydrocarbon productivity [9]. Therefore, expanding the cobalt-based catalysts life catalyst life enhances the economy of the FT process; although catalyst regeneration or replacement is necessary as well.

Numerous investigations on cobalt catalysts deactivation mechanisms have been led to original articles [9-32] as well as some reviews [33-36]. The main mechanisms of deactivation comprise poisoning [18-22], carbon or hydrocarbon deposition [9,19,20,23,25,27,30,31], sintering [14,19,25,29,32], catalyst-support compound formation [14,19,26], catalyst re-oxidation [10,12-15,19,26,32], and mechanical cause like attrition [27]. Poisoning can be prevented by robust syngas clean up. Moreover, other aforementioned mechanisms like re-oxidation can be avoided through forming specific cobalt crystallites sizes [16,17] or careful control of the reactor partial pressures of hydrogen and water [17]. Regarding catalyst-support compound formation, Moodley *et al.* [26] indicated that small amounts of cobalt aluminate formation does not

*Corresponding author. E-mail: h.ateshy@hamoon.usb.ac.ir

influence the deactivation of cobalt catalysts in realistic FTS conditions (P_{H2O}/P_{H2} = 1-1.5, P_{H2O} = 4-6 bar). Furthermore, the results of [30] suggest that Pt and Ru promoters lead to decline in C and C compound formation on the Co surface.

Operating conditions along with catalyst structure influence catalyst deactivation rate. Pena *et al.* [31] investigated the effect of different gas-space velocities and H_2/CO ratios on the amounts of deposed carbon species in a continuously stirred tank reactor (CSTR) at total pressure of 20 bar. They stated that for H_2/CO = 2, only very small amounts of strongly adsorbed hydrocarbons and polymeric carbon were detected while lower H_2/CO ratio and lower gas space velocity result in larger amounts of deposed carbon species. Reporting carbon deposition as the only deactivation mechanism, Keyvanloo *et al.* [9] have succeeded to eliminate the other mechanisms through modifying the catalyst structure, imposing particular reduction conditions, and setting out specific operating conditions.

A deactivation rate, involved in FT rate expression, can amazingly enhance the accuracy of kinetic calculation. Thus, deactivation modeling will help refiners reduce its operational costs by not only easily control catalytic processes, but also run FTS at the optimized process conditions. Although deactivation issues like mechanisms, reactivation, and extent have been widely explored, in most reviewed studies on catalyst activity, deactivation rates were not addressed quantitatively. Considering the few studies which have presented unrealistic simple power law expressions (SPLEs) [19,37] and more reliable generalized power law expressions (GPLEs) [38-40], deactivation modeling of cobalt FT catalyst deserves further investigations. The SPLEs predict zero activity for a long time on stream, while catalyst activity during FTS on cobalt typically tends to a limited activity of 0.3-0.5 [38]. More consistent results of GPLEs provide a realistic vision of cobalt FT catalyst deactivation; it, however, cannot be applicable in all cases. A full detailed discussion will be presented later.

With the aim of providing a more realistic contribution to the FT catalyst deactivation rate modeling, the main objective of this work is to offer a well-fitted sigmoid model with incredibly meaningful parameters, which provide us a fascinating insight into the nature of catalyst deactivation. Note that the proposed novel model has not been addressed elsewhere.

THEORY

A quite common belief amongst researchers has been stablished regarding deactivation profile of FT catalysts that follows a decreasing trend, as depicted in Fig. 1. Numerous reports, however, have shown different patterns [10,11,22,23]. Therefore, the introduction of a comprehensive model to represent all possible situations seems to have been of importance for FT community which is presented in the following section.

Model Introduction

A state-of-the-art sigmoid model is introduced to fit the cobalt-based FT catalysts deactivation trend. The sigmoid function is a mathematical model which has been widely employed to simulate the natural life cycle of many important events, from biological organisms, to schools and companies, marriages, careers, growth of tumors, or economics and sociology. In chemical reaction engineering, the sigmoidal pattern may be used for autocatalytic reactions in which one of the products of reaction acts as a catalyst. The simplest such reaction is:

$$A + B \Leftrightarrow B + B \tag{1}$$

In autocatalytic reaction the graph of conversion of A versus time follows a sigmoidal pattern as shown in Fig. 2.

Considering the various implications of sigmoid function, with a proper amendment, the modified sigmoid model can be utilized to mimic the catalyst deactivation lifetime. The main distinctive feature of sigmoidal fit for catalyst deactivation is that, unlike previous models, it can precisely predict the majority of catalyst failure rate during FTS with its incredible meaningful parameters. Moreover, the given clear imaging by the model parameters provides a realistic intuition into the catalyst activity. Additionally, sigmoid function estimates steady-state activity at infinite time which traditional power law deactivation rate expressions fail to predict. Specifically, the catalyst activity may be modeled by using the following expression:

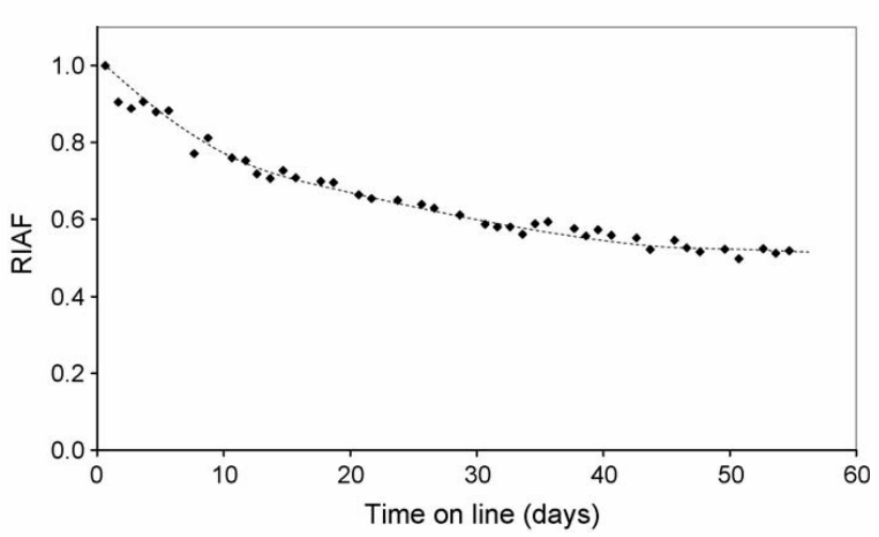

Fig. 1. Relative intrinsic activity factor (RIAF) for a Co/Pt/Al_2O_3 catalyst during FTS [16].

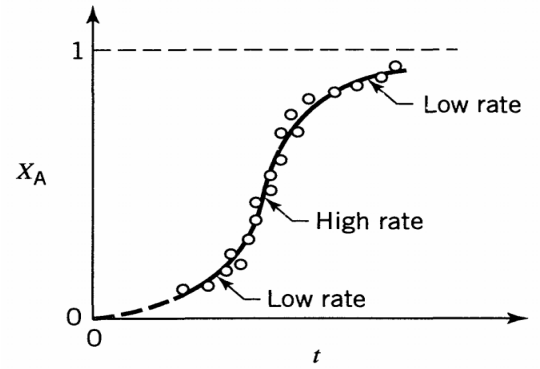

Fig. 2. Rate *versus* time plot for an autocatalytic reaction [5].

$$a = a_{SS} + \frac{a_L}{1+e^{k(t-t_{ip})}} \quad (2)$$

where a, a_{SS}, a_L, t_{ip} and k stand for catalyst activity at time t, steady-state activity, an approximation of total activity loss, time at the inflection point where the catalyst experiences its highest deactivation rate, and the speed of activity loss, respectively. The parameter k can be considered as a kind of deactivation kinetic constant, since increase in k leads to a rise in the deactivation rate, as indicated in Fig. 3ii. Note that in Eq. (2) the dimension of k is 1/s while a_{SS}, a and a_L are dimensionless parameters. Figure 3i schematically shows Eq. (2) illustrating catalyst activity *vs*. time and Fig. 3ii displays the deactivation rate which is the differentiation of Eq. (2).

In cases like Fig. 1, the curve commences after the inflection point resulting in a negative value of t_{ip}. The model parameters can be defined through mathematical calculations to find the inflection point as well as the curve height which indicates the activity loss. In order to obtain the inflection point we need the second derivative of the function to set it equal to zero, as follows:

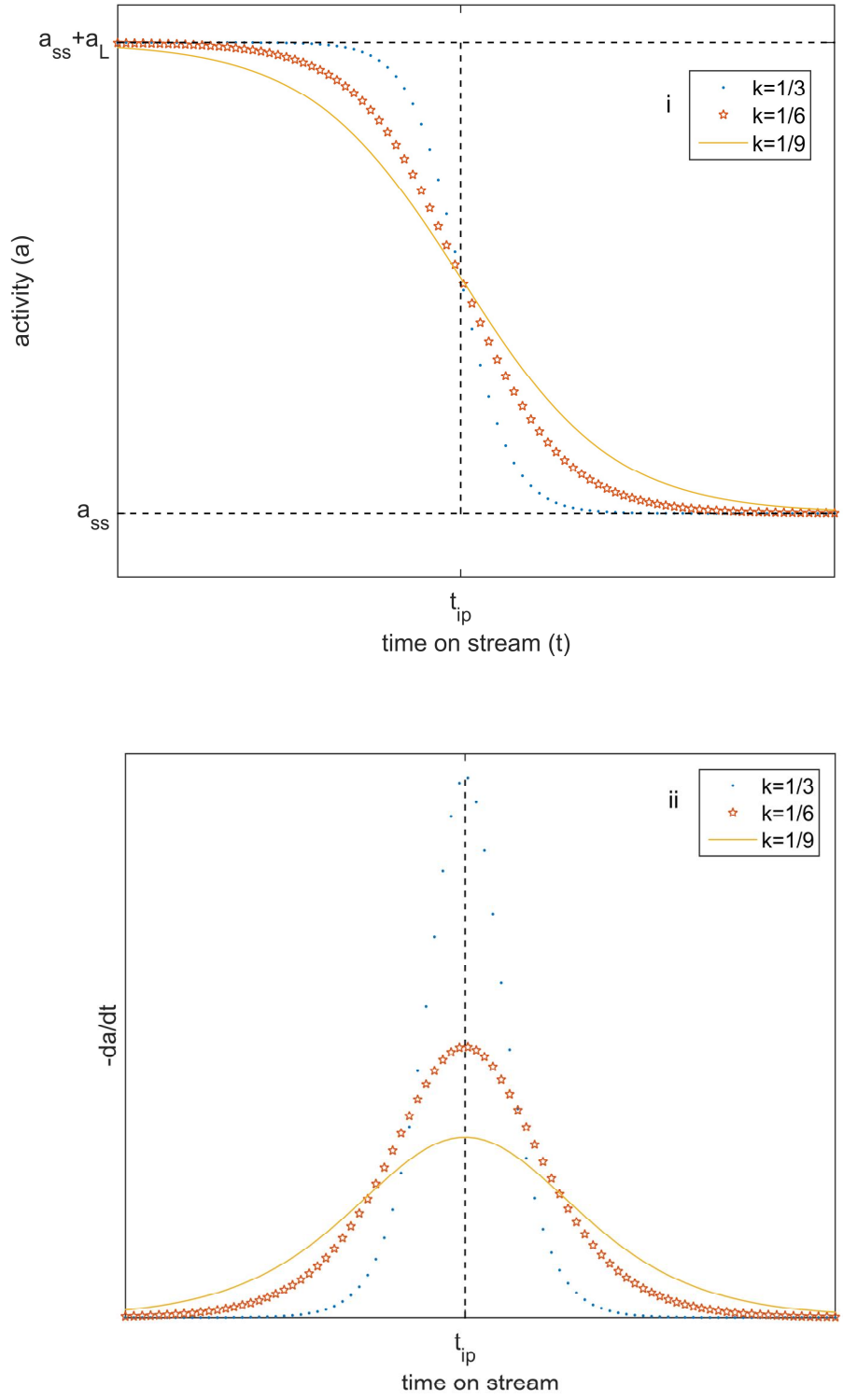

Fig. 3. schematic of (i) activity-time data as sigmoid equation as well as (ii) the deactivation rate.

$$\frac{da}{dt}=\frac{d}{dt}\left(a_{SS}+\frac{a_L}{1+e^{k(t-t_{ip})}}\right)=a_L\left(\frac{0-ke^{k(t-t_{ip})}}{\left(1+e^{k(t-t_{ip})}\right)^2}\right)\Rightarrow\frac{da}{dt}=-a_L\frac{ke^{k(t-t_{ip})}}{\left(1+e^{k(t-t_{ip})}\right)^2}$$

$$\frac{d^2a}{dt^2}=\frac{da}{dt}\left(-a_L\frac{ke^{k(t-t_{ip})}}{\left(1+e^{k(t-t_{ip})}\right)^2}\right)=-a_Lk\left(\frac{ke^{k(t-t_{ip})}\left(1+e^{k(t-t_{ip})}\right)^2-2e^{k(t-t_{ip})}\left(1+e^{k(t-t_{ip})}\right)ke^{k(t-t_{ip})}}{\left(1+e^{k(t-t_{ip})}\right)^2}\right)=0$$

$$\Rightarrow\left(1+e^{k(t-t_{ip})}\right)-2e^{k(t-t_{ip})}=0\Rightarrow1+e^{k(t-t_{ip})}=2e^{k(t-t_{ip})}\Rightarrow e^{k(t-t_{ip})}=1\Rightarrow t=t_{ip} \quad (3)$$

So, the inflection point of the model is t_{ip}. To calculate the curve height, the difference between activity at $t = 0$ and $t\to\infty$ should be obtained, as below:

$$\text{curve height}=\text{a}(0)-\text{a}(\infty)=\lim_{t\to0}\left(a_{SS}+\frac{a_L}{1+e^{k(t-t_{ip})}}\right)-\lim_{t\to\infty}\left(a_{SS}+\frac{a_L}{1+e^{k(t-t_{ip})}}\right)$$

$$\Rightarrow\text{curve height}=a_{SS}+\frac{a_L}{1+e^{-kt_{ip}}}-a_{SS}=\frac{a_L}{1+e^{-kt_{ip}}} \quad (4)$$

Since the term $e^{-kt_{ip}}$ is often near to zero so the curve height or activity loss can be assumed as:

$$\Rightarrow\text{curve height}=\frac{a_L}{1+e^{-kt_{ip}}}\cong a_L \quad (5)$$

Model Elucidation

Having three sections, the curve is principally an extended s shape lying on its side. Regarding catalyst deactivation, firstly there is a section in which the curve smoothly declines depending on the catalyst structure, feed composition, operating conditions, and many other factors. This section corresponds to the initial period of FT process in which two fundamental phenomena occur: further activation after reduction with H_2 and deactivation. The observed increase in activity is generally associated with reduction of CoO to Co metal in the presence of both CO and H_2 and restructuring (roughening) of the surface. Moreover, carbidization (formation of cobalt carbide (Co_2C)) may favor the catalyst activity as reported in the literature that suggest catalytic properties of cobalt carbide [42,43]. Accordingly, slow drop in catalyst activity at first may be attributed to the counteractive effect of further activation after reduction with H_2 and primary deactivation mechanisms including oxidation or sintering.

The second section, which can be called as the steep section, associates with a strictly falling line in the elongated S shape. The duration of this section is defined by k which is an indicator of the deactivation kinetic in the main period of deactivation. During this section, sintering, carbon deposition [20], and maybe oxidation [17] are the major mechanisms resulting in a higher catalyst deactivation rate. The point t_{ip}, which is recognized as inflection point, indicates that the catalyst deactivation rate starts declining toward a limiting activity.

The third phase of the curve is again slightly declining and reaching a limit. In this section, the curve proceeds toward a constant activity indicating that the system tends to a thermodynamic equilibrium in which there is no driving force for spontaneous changes in mechanical, chemical, and thermal state of the system. At the end of the curve, the catalyst reaches the steady-state activity and no further deactivation occurs.

Two apparent deactivation regimes can be considered in the catalyst lifetime. The first short-term initial deactivation regime (A in Fig. 4) is linked with reversible deactivation, while the second long-term regime (B in Fig. 4) is associated with irreversible deactivation [34]. The inflection point obtained from the proposed sigmoid model approximately predicts where the first regime ends and the second regime starts, which could be vital for the process design in industrial applications.

In petrochemical companies where all the equipment is designed based on a constant product flow rate of the reactor operating at a defined conditions, catalyst deactivation causes the conversion to decline. Therefore, the product flow rate decreases. A deactivation model embedded in control package installed there help the system manages the product flow rate based on the catalyst failure rate. Clearly, a deactivation model helps monitoring the catalyst decline and further strategy can be planed, whether a regeneration process or temperature increase in order to maintain a constant catalyst activity.

As the catalyst activity-time data was considered to start from one, so the regression results should be obtained in a way that satisfy the following equation: $a_{SS}+a_L\approx1$. By using the sigmoid equation parameters, the nature of catalyst deactivation can be interpreted. For example, closer a_{SS} to one or lesser values of a_L indicates that at a long

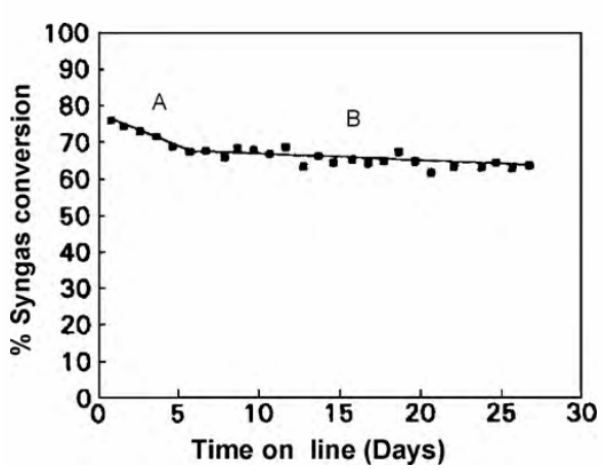

Fig. 4. Typical cobalt FT catalyst lifetime [34].

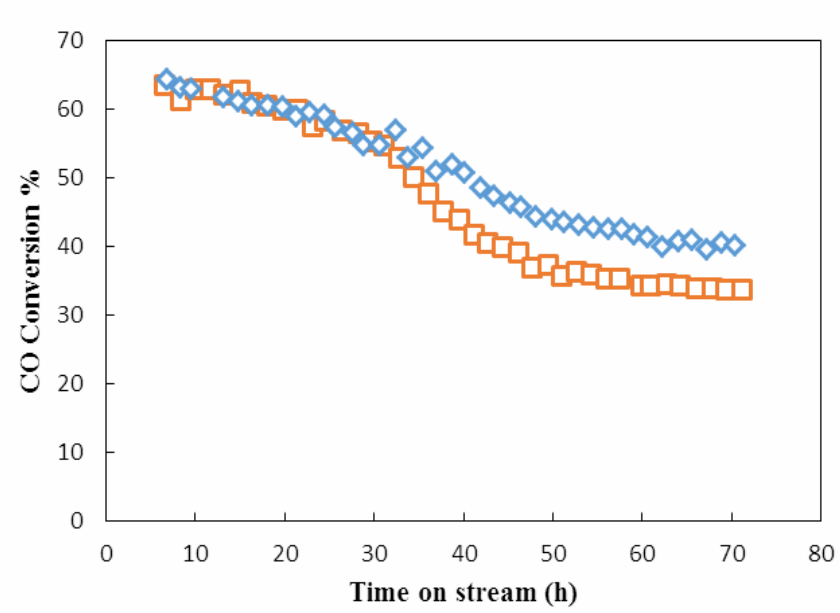

Fig. 5. Conversion of CO with time on stream, (a) without CO_2 addition (b) with CO_2 addition. Reaction conditions: P = 20 bar, T = 220 C, SV = 2000 L/kg_{cat}/h and H_2/CO = 2 [10].

period of time, the catalyst reaches a higher constant activity or shows more stability during the process. Likewise, a_L shows how much the catalyst loses its activity. Moreover, t_{ip} illustrates the time when the deactivation rate starts to decline. The amount of t_{ip} reveals the time for a catalyst to reach the highest deactivation rate. Finally, a catalyst with higher k and higher t_{ip} exhibits more stability and resistance to deactivation in the first section. The higher the k is, the smaller the steep section would be.

Furthermore, the effect of different factors on deactivation of the catalyst in FT process can be compared *via* the obtained model parameters. Suppose that we have fitted two activity-time data for two different catalysts in the same reactor and similar operating conditions. The steady-

state activity (a_{SS}), the amount of activity loss (a_L), the time of highest deactivation rate along with the maximum deactivation rate (t_{ip}, k) for the two catalysts can be compared quantitatively. The t_{ip} and k constants provide useful criteria for evaluating the stability of the catalyst at the beginning of the FT process. Accordingly, as t_{ip} and k rise, it can be concluded that synthetized catalyst or imposed operating conditions result in more stability and thus higher production rate in the first section. Ultimately, Eq. (6) shows how much percentage the catalyst or operating conditions 2 change the deactivation rate ($dr\%$) of catalyst or operating conditions 1.

$$dr\% = \frac{k_2 - k_1}{k_1} \times 100 \tag{6}$$

DATA PREPROCESSING

Nine sets of experimental FT catalyst activity-time data were borrowed from the literature to be modeled through sigmoidal pattern. The Kim *et al.* experiment [10] is the first case study used for modeling. They investigated the effect of adding CO_2 into the reactor operating the FT process in a fixed-bed reactor under typical FTS conditions; 220 °C, 20 bar, and SV ($L/kg_{cat}/h$) = 2000. The activity test data were collected using the two reactant gas mixtures, $H_2/CO/Ar$ and $H_2/CO/CO_2/Ar$ with 20% CO_2. They reported that the addition of CO_2 slightly oxidized the reduced $Co/\gamma\text{-}Al_2O_3$ destroying a fraction of active sites leading to more deactivation of the catalyst, as evident in Fig. 4.

The second case study was conducted by Park *et al.* [11], who studied the catalytic performance of cobalt-based catalyst with phosphorous-modified alumina support ($P\text{-}Al_2O_3$) and promoted with Pt or Ru during the FT process. They utilized a slurry-phase continuous-stirred tank reactor for 1000 h time on stream under the following reaction conditions: liquid medium (squalane) = 300 g, catalyst = 5.0 g, T = 230 °C; P=20 bar, space velocity (SV; $L/kg_{cat}/h$) = 2000, and feed composition of $H_2/CO/CO_2/Ar$ = 57.3/28.4/9.3/5.0 mol%. Since the process has reached steady-state condition after about 50 h, time on stream between 110 h and 1000 h was eliminated. They reported that Pt promoted catalyst had performed much more stable than others ($Co/P\text{-}Al_2O_3$ and $Ru/Co/P\text{-}Al_2O_3$). However, we only consider the data of $Co/P\text{-}Al_2O_3$ and $Pt/Co/P\text{-}Al_2O_3$ for regression. Figure 5 shows the conversion *vs*. time on stream data of park *et al.* [2] experiments on $Co/P\text{-}Al_2O_3$ and $Pt/Co/P\text{-}Al_2O_3$ catalysts.

In the third attempt, the experimental data of Karaca *et al.* [25] was considered. They investigated the catalytic performance of two different synthetized Pt-promoted Co/Al_2O_3. The catalysts involved the same content of Pt and Co but different cobalt precursor: nitrate and acetate. The first was named $CoPt/Al_2O_3$-N and the second was indicated as $CoPt/Al_2O_3$-A. Moreover, the calcination step was performed at 573 K for $CoPt/Al_2O_3$-A and $CoPt/Al_2O_3$-N1 and 773 K for $CoPt/Al_2O_3$-N2. They stated that catalyst calcination at 773 K instead of 573 K does not have a remarkable impact on the size of supported Co_3O_4 crystallites while utilizing cobalt acetate as a precursor considerably reduces the cobalt particle size. Afterwards, catalytic performance tests of $CoPt/Al_2O_3$-A and $CoPt/Al_2O$-N1 were conducted under syngas flow in a capillary reactor at 493 K and 20 bar, shown in Fig. 6. As an important result, they concluded that the observed lower catalytic activity of the $CoPt/Al_2O_3$-A catalyst (cobalt acetate as precursor) could be connected to lower reducibility of smaller cobalt particles and consequently lower concentration of cobalt active sites.

For the fourth case study, the work of Park *et al.* [27] was considered. They studied the catalyst deactivation by the formation of aggregated catalyst lumps of the phosphorous-modified cobalt-alumina ($Co/P\text{-}Al_2O_3$), unmodified cobalt-alumina (Co/Al_2O_3), phosphorous-modified Pt-promoted cobalt-alumina ($Pt/Co/P\text{-}Al_2O_3$), and the unmodified Pt-promoted cobalt-alumina ($Pt/Co/Al_2O_3$) catalysts in CSTR under the following reaction conditions: liquid medium (squalane) = 300 g, catalyst = 5.0 g, T = 230 °C, P = 20 bar, space velocity (SV; $L/kg_{cat}/h$) = 2000, feed composition of $H_2/CO/CO_2/Ar$ = 57.3/28.4/9.3/5.0 mol%. They reported that the catalytic activity of the Pt-promoted catalysts is much higher compared to the unpromoted ones. For the Pt-promoted catalysts considered for regression in this article, the higher activity at the beginning of the process with a fast deactivation rate and smaller steady-state activity can be observed for $Pt/Co/Al_2O_3$ catalyst, as illustrated in Fig. 7.

It is important to mention that the starting point data in

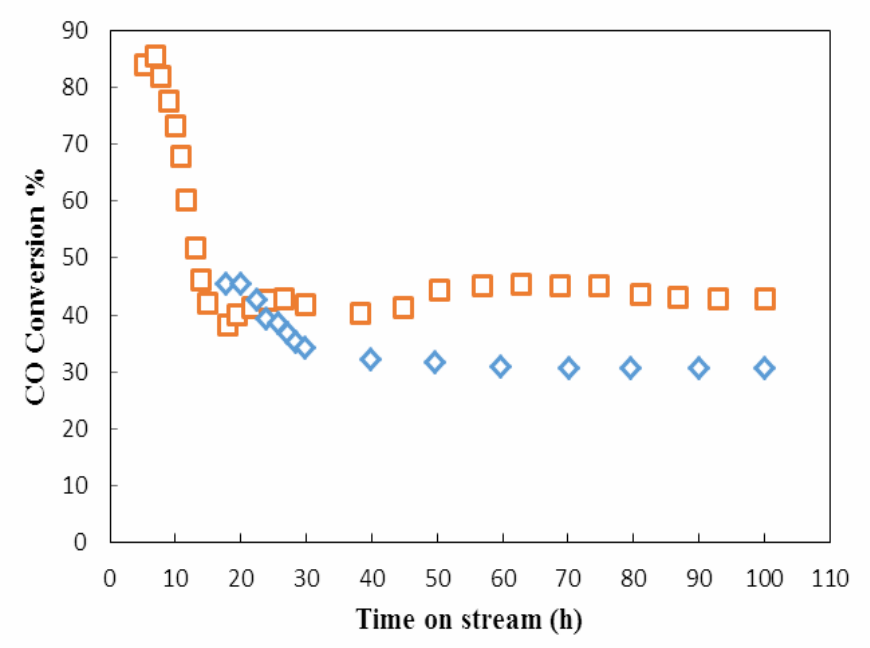

Fig. 6. Conversion of CO with time on stream for (a) Pt/Co/P-Al_2O_3 and (b) Co/P-Al_2O_3 catalyst. Reaction conditions: catalyst = 5.0 g; T = 230 °C; P = 2.0 MPa; space velocity (SV; L/kg_{cat}/h) = 2000; and feed composition of H_2/CO/CO_2/Ar = 57.3/28.4/9.3/5.0 mol% [11].

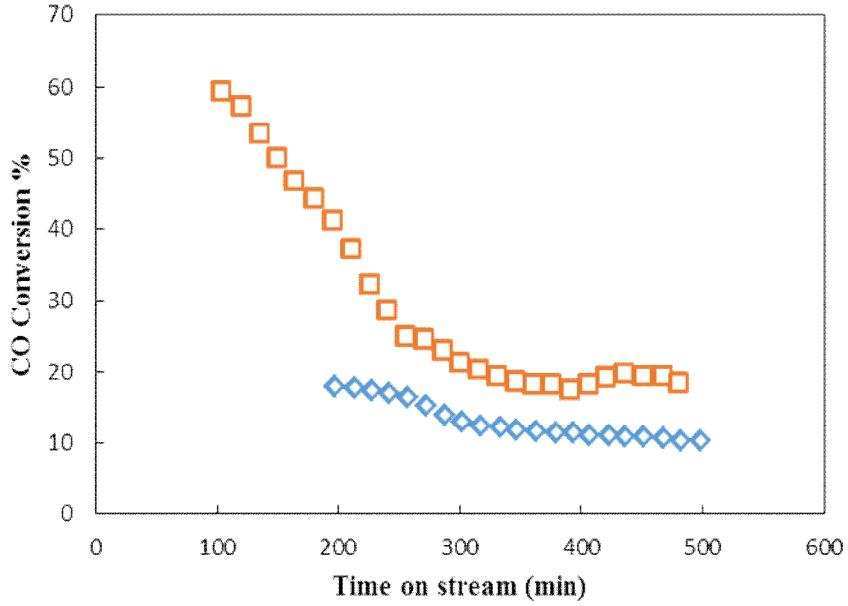

Fig. 7. Conversion of CO with time on stream for (a) CoPt/Al_2O_3-N1 and (b) CoPt/Al_2O_3-A catalyst. Reaction conditions: (T = 493 K, P = 20 bar, H_2/CO = 2 and GHSV = 25,000 ml g^{-1} h^{-1} for CoPt/Al_2O_3-N1 and GHSV = 19,600 ml g^{-1} h^{-1} for CoPt/Al_2O_3-A) [12].

Figs. 4 to 7 is the highest conversion point and assumed a = 1. Clearly, the initial catalytic test data in which the catalyst activity hits a peak was removed. In order to show the capability of the proposed model for the long-term deactivation period, Fig. 1 was considered as the last case study. The regression results will be presented in the next section.

RESULTS AND DISCUSSION

The main motivation behind the present study is to propose a robust and realistic model with meaningful parameters for catalyst deactivation rate in the FT process. The activity of the catalyst was calculated as:

$$a = \frac{X_t}{X_0} \tag{7}$$

where X_0 denotes the CO conversion at the beginning of the process and X_t indicates the CO conversion at any time. As mentioned, nine experimental data sets of catalyst CO conversion from four references [10,11,16,25,27] were analyzed in this study. Note that the curve fitting toolbox of MATLAB R2014b was used and the Levenberg-Marquardt algorithm was chosen for the regressions.

Case Study 1

In Figs. 8-11 the experimental data are denoted by open symbols, while sigmoidal fit predictions are shown as solid lines. Figure 8 shows activity-time data of Kim *et al.* [10] representing the influence of CO_2 on the activity of Co/γ-Al_2O_3 catalyst in FTS. The regression results show that the addition of 20% mole CO_2 into the system causes to about 7% growth of the activity loss of the catalyst. Moreover, the higher amount of k in with-CO_2 run compared to without-CO_2 run indicates that addition of CO_2 increases the rate of catalyst deactivation. The CO_2 effect on the catalyst deactivation rate can be estimated quantitatively by using *dr%* as follows:

$$dr\% = \frac{k_2 - k_1}{k_1} \times 100 = \frac{0.1592 - 0.0934}{0.0934} \times 100 = 70.45\% \tag{8}$$

So, the 20% presence of CO_2 in the feed stream leads to around 70% increase in k or increase in the deactivation rate. However, no remarkable change in t_{ip} beside 70% increase in k in with-CO_2 run shows that the catalyst stability in the first section of the sigmoidal fit was affected by CO_2.

Case Study 2

The second case study concerns to the Park *et al.* [11] experiment investigating the effect of Pt as a metal promoter of the catalyst. The regression results show faster deactivation rate (lower t_{ip} and higher k) for Pt-promoted catalyst, displayed in Fig. 9. However, Fig. 5 reveals that Pt-promoted catalyst converts much more CO at the beginning of the process and reaches a higher CO conversion at steady-state time. The effect of Pt on the deactivation rate can be estimated as:

$$dr\% = \frac{k_2 - k_1}{k_1} \times 100 = \frac{0.803 - 0.3126}{0.3126} \times 100 = 156.88\% \tag{9}$$

So, despite increase in CO conversion, the deactivation rate was intensified one and a half times more in the Pt promoted catalyst.

Case Study 3

Third data set was borrowed from Karaca *et al.* [25] who examined the effect of cobalt precursor on catalytic activity of the Pt-promoted cobalt-alumina. Figure 10 depicts the regression result indicating that the deactivation rate for the catalyst with smaller cobalt particle ($CoPt/Al_2O_3$-A) is faster while the steady-state activity is much higher compared to the catalyst with larger cobalt particles. However, Fig. 6 illustrates that larger cobalt particles in catalyst significantly enhance the CO conversion and result in a higher steady-state conversion of CO. Ultimately, the effect of cobalt oxide crystallites diameter on the deactivation rate, which is about twice in $CoPt/Al_2O_3$-N1 (adapted from Table 1 of reference [25]), can be calculated as follows:

$$dr\% = \frac{k_2 - k_1}{k_1} \times 100 = \frac{0.0238 - 0.0313}{0.0313} \times 100 = -23.96\% \tag{10}$$

So, despite the improvement in CO conversion, increase in cobalt oxide crystallites diameter causes an almost 24%

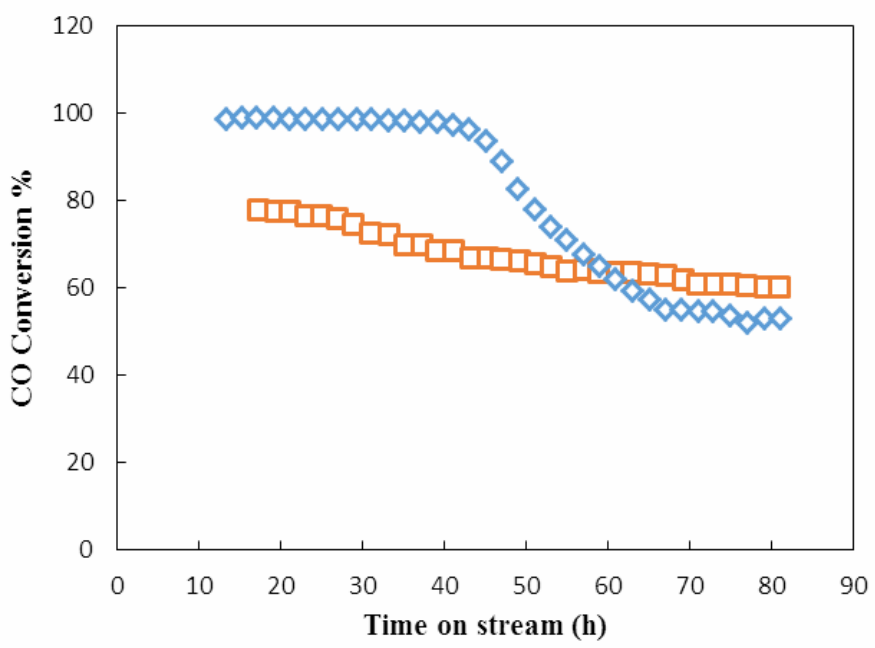

Fig. 8. Conversion of CO with time on stream for (a) Pt/Co/P-Al_2O_3 and (b) Pt/Co/Al_2O_3 catalysts. Reaction conditions: T = 230 °C, P = 2.0 MPa, SV (l/kgcat/h) = 2000, feed composition (H_2/CO/CO_2/Ar; mol%) = 57.3/28.4/9.3/5.0 [13].

drop in the deactivation rate. However, the steady-state activity is significantly affected by increase in cobalt oxide crystallites diameter; *i.e.,* the steady-state activity was halved with cobalt oxide crystallites diameter being doubled.

Case Study 4

In the fourth case study, the data of Park *et al.* [27] study was considered. Two of the four catalysts investigated by them were modeled in this study providing quantitative exploration of the effect of phosphorous-modification of Pt-promoted cobalt alumina catalyst. Like previous case studies, the regression results in brilliant consequences with precise prediction of catalyst lifetime indicating that phosphorous-modification significantly reduces the maximum deactivation rate of Pt-promoted cobalt alumina catalyst as well as improvement in steady-state activity, as shown in Fig. 11. However, considering Fig. 7, it is observed that Pt/Co/Al_2O_3 catalyst converts much more CO than Pt/Co/P-Al_2O_3 until 40 h time in line indicating the higher catalyst stability until the inflection point which can be realized by the higher amount of t_{ip} and higher value of k; while it reaches a lower steady-state CO conversion. In other words, Pt/Co/Al_2O_3 shows more stability in the first section. Furthermore, the variation of deactivation rate by phosphorous-modification of the catalyst can be calculated *via* Eq. (6).

$$dr\% = \frac{k_2 - k_1}{k_1} \times 100 = \frac{0.0641 - 0.2258}{0.2258} \times 100 = -71.61\% \qquad (11)$$

So, phosphorous-modification of the Pt/Co/Al_2O_3 catalyst plummets the deactivation rate of the catalyst by around 72% and significantly enhance the steady-state activity.

Case Study 5

The capability of the proposed model for short-term deactivation has been visually confirmed and then proved *via* statistical criteria. Since the FT community seeks for a long-term deactivation model, the Saib *et al.* [16] long-term experiment was considered for the last case study. They

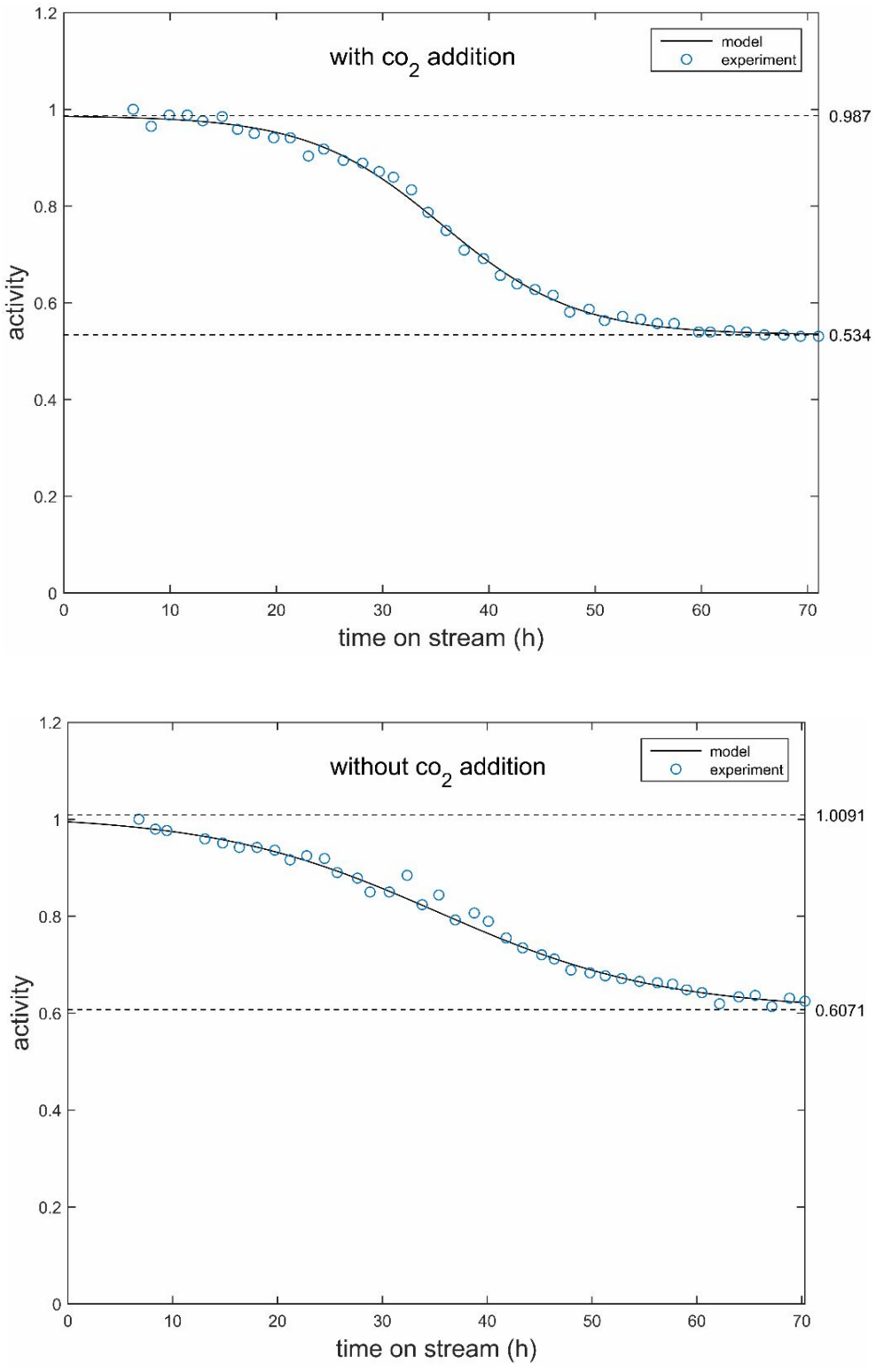

Fig. 9. Sigmoidal fit of activity-time data of Co/γ-Al_2O_3 catalyst for Kim *et al.* [10] experiment.

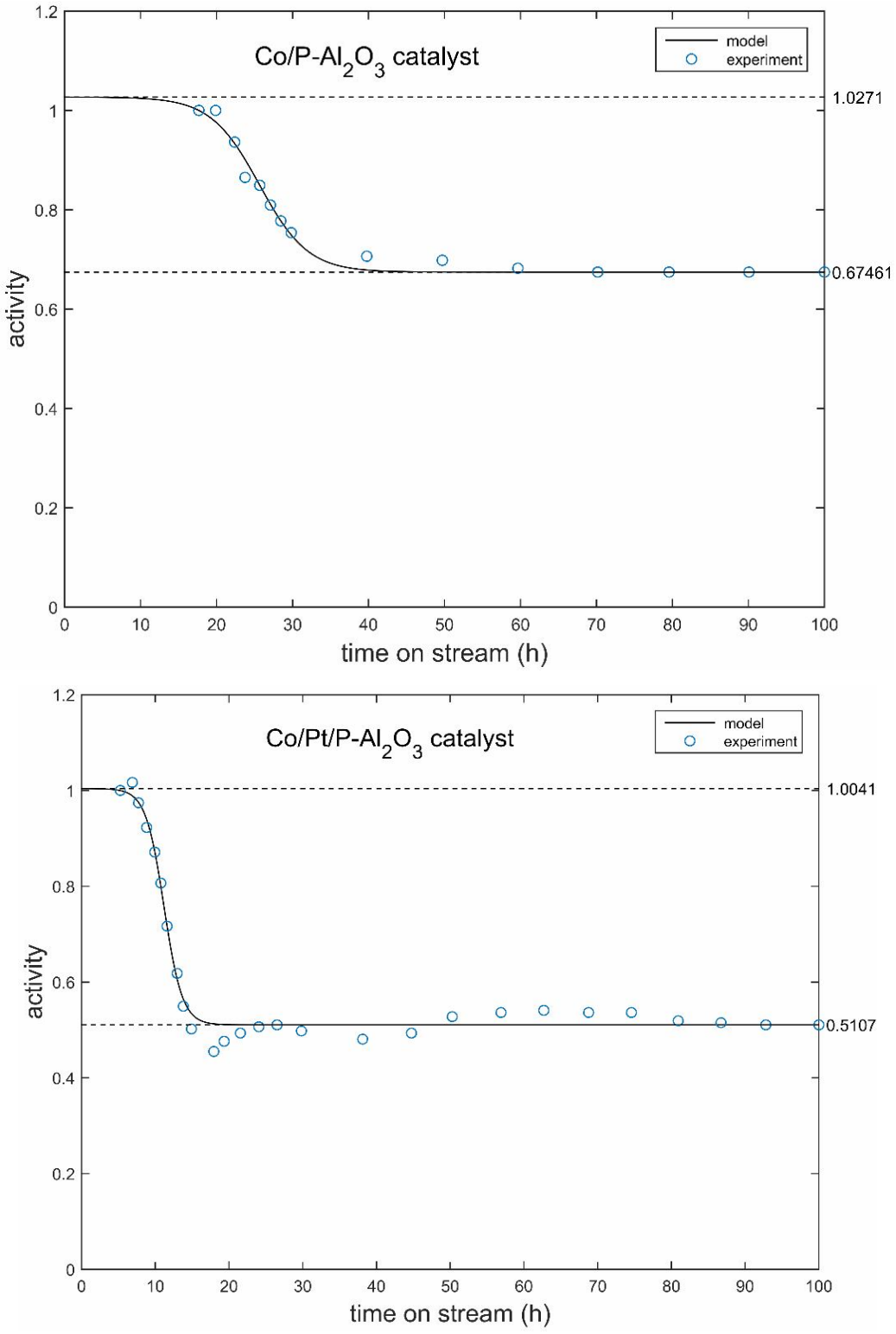

Fig. 10. Sigmoidal fit of activity-time data of Park *et al.* [11] experiment.

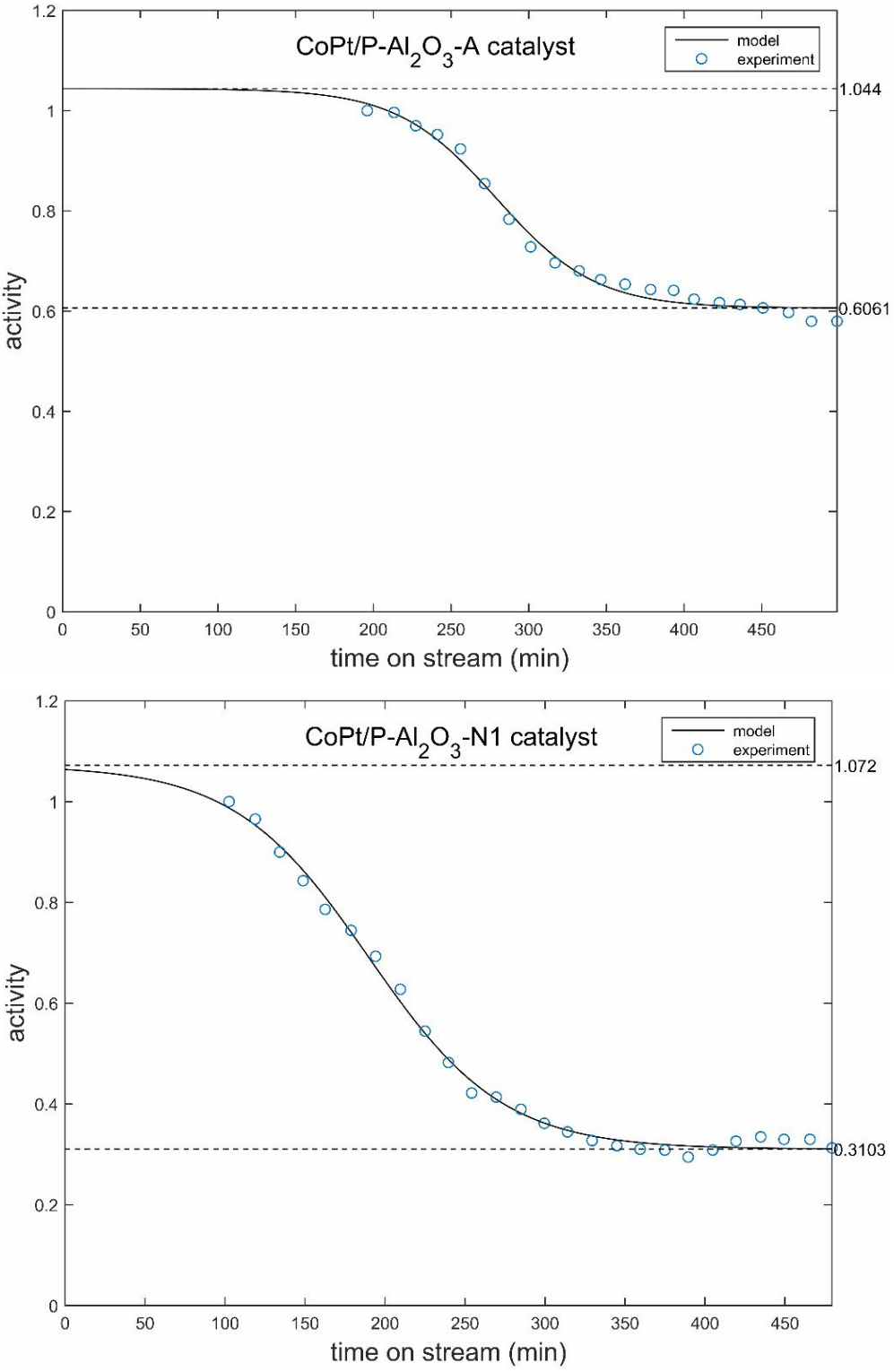

Fig. 11. Sigmoidal fit of activity-time data of Karaca *et al.* [12].

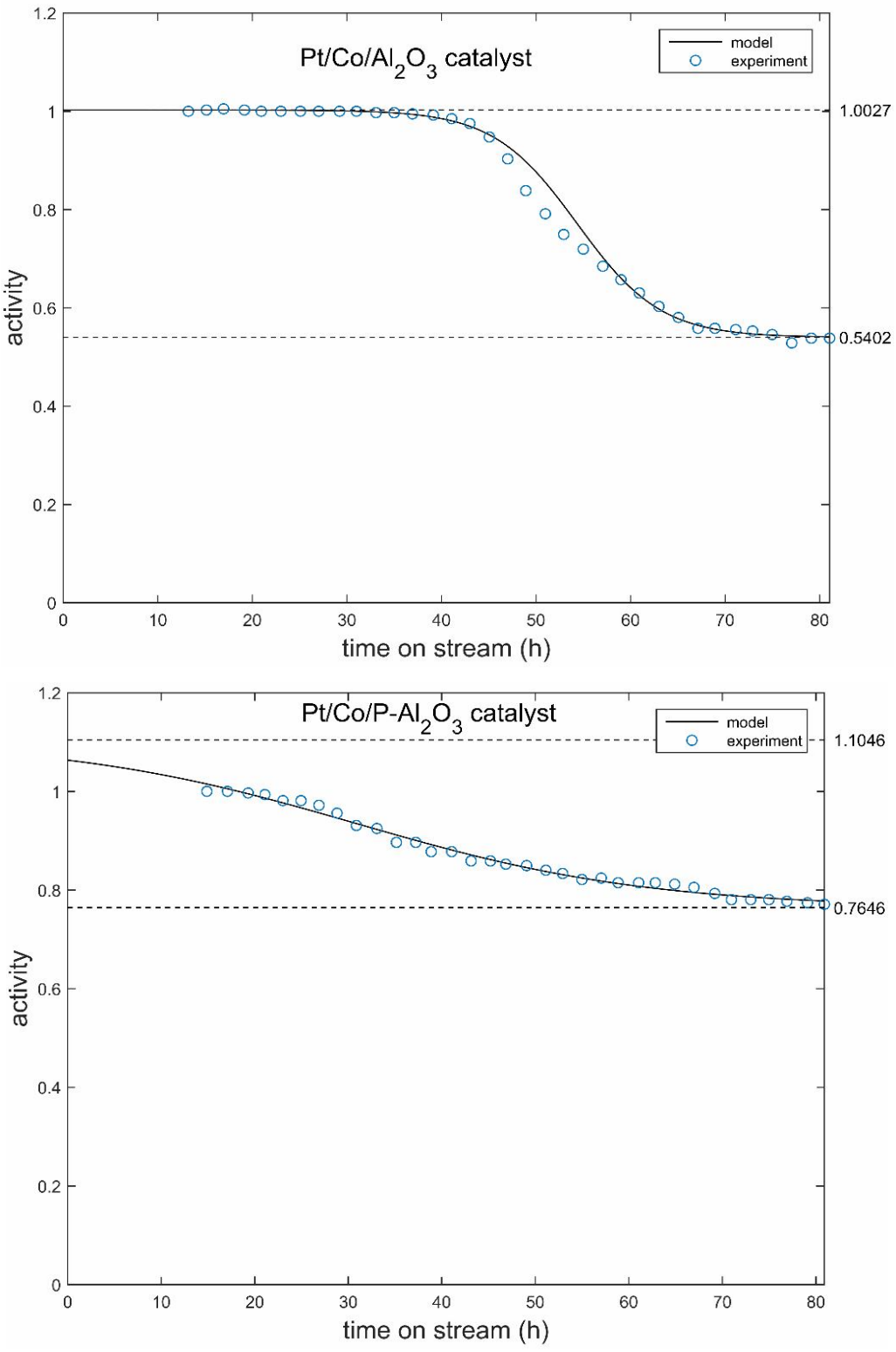

Fig. 12. Sigmoidal fit of activity-time data of Park *et al.* [13].

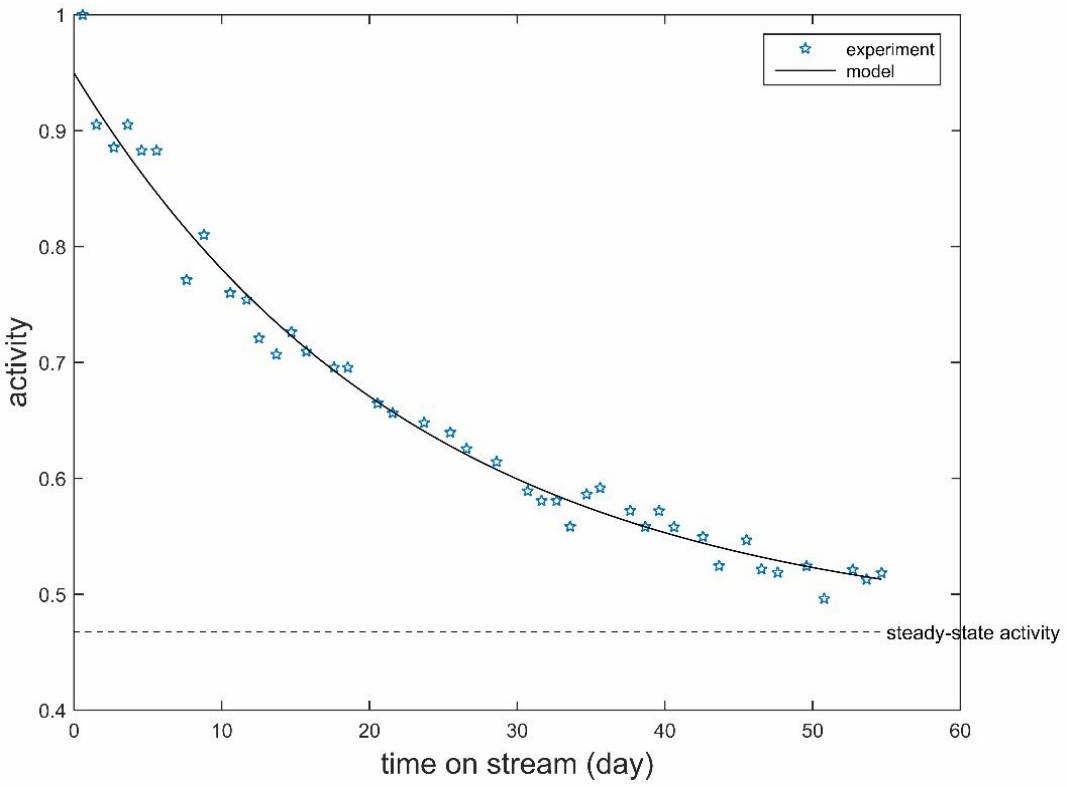

Fig. 13. Sigmoidal fit of activity-time data of Saib *et al.* [4].

examined $Co/Pt/Al_2O_3$ catalyst during realistic Fischer-Tropsch synthesis, *i.e.,* 230 °C, 20 bar, (H_2 + CO) conversion between 50 and 70%, feed gas composition of *ca*. 50 vol.% H_2 and 25 vol.% CO, P_{H_2O}/P_{H_2} =1-15, P_{H_2} = 4-6 bar, as depicted in Fig. 1. The regression results endorse the introduced sigmoid model for the long-term deactivation period of cobalt FT catalyst with two big differences in comparison to the previous case studies: a_L and t_i. Since only the last section of the proposed sigmoid model captures the data of ref. [16] (Fig. 12), the a_L and t_i parameters currently fail to be intuitively interpreted unless the data of initial rise are considered. However, the wonderful predictions *via* the model can be extensively applied for control purposes.

As visually confirmed, the proposed sigmoid model seems to cover the activity-time data in many occasions whether short-term or long-term deactivation period, while the GPLEs models do not have such capability.

Table 1 represents the regression and Goodness-of-fit statistic results including R-square, adjusted R-square, Sum of Squares Due to Error (SSE), and Root Mean Squared Error (RMSE). Capability of the proposed sigmoid model in precise prediction of the activity for cobalt FT catalyst lifetime in typical operating conditions (T = 220 °C, P = 20 bar, and H_2/CO = 2) can be perfectly demonstrated through four sets of statistics.

Table 2 summarizes the type of reactor, reaction conditions, CO conversion at the beginning of the process (X_0), and run durations of experimental data used in this study.

As indicated in data preprocessing section, the activity-time data may exhibit more stability at the beginning rather than the middle of the FT reaction. In such cases the first and second order GPLEs seem to be inappropriate for modeling the catalyst deactivation trends, since they are only able to predict a monotonic deactivation rate without

Table 1. Deactivation Rate Parameters for Sigmoid Equation and Goodness-of-fit Statistics

Case study	Ref.	Catalyst	Sigmoid equation parameters				Goodness-of-fit statistics			
			a_{SS}	a_L	t_{ip}	k	SSE	R-square	Adjusted R-square	RMSE
1	[10]	Co/γ-Al_2O_3[a]	0.534	0.453	35.64	0.1592	0.004768	0.9962	0.9959	0.01151
1	[10]	Co/γ-Al_2O_3[b]	0.6071	0.402	35.36	0.0934	0.004277	0.9933	0.9928	0.0109
2	[11]	Pt/Co/P-Al_2O_3	0.5107	0.4934	11.19	0.803	0.01211	0.986	0.9842	0.02295
2	[11]	Co/P-Al_2O_3	0.6746	0.3525	25.63	0.3126	0.002278	0.9886	0.9855	0.01439
3	[12]	CoPt/Al_2O_3-A	0.6061	0.4379	279.2	0.0313	0.004774	0.9894	0.9876	0.01676
3	[12]	CoPt/Al_2O_3-N1	0.3103	0.7617	189.8	0.0238	0.006849	0.995	0.9943	0.01764
4	[13]	Pt/Co/Al_2O_3	0.5402	0.4624	54.35	0.2258	0.001887	0.9986	0.9984	0.007803
4	[13]	Pt/Co/P-Al_2O_3	0.7646	0.34	30.94	0.0641	0.002259	0.9886	0.9874	0.008677
5	[4]	Co/Pt/Al_2O_3	0.4676	213.2	-140.7	0.0433	0.01096	0.9848	0.9836	0.01698

[a]Experiment with CO_2 stream. [b]Experiment without CO_2 stream.

an inflection point in the catalyst lifetime like the ones presented in this work.

Statistical Interpretation

Due to almost the same time on stream for the case studies 1, 2 and 4, the averages and standard deviations of these case studies were calculated, which are presented in Table 3.

The results in Table 3 demonstrate that for typical process conditions including temperatures in the range of 220-230 °C, pressures of 20 bar, and H_2/CO ratio of 2, the average of the deactivation rate constants of the model are $a_{SS} = 0.6 \pm 0.1$ and $a_L = 0.42 \pm 0.06$. Steady-state (asymptotic) activities are largely in the range of 50-70% of initial activity based on the extrapolation of sigmoid function. Additionally, R-square and adjusted R-square endorse the performance of the sigmoid function for deactivation data. This consistency is exciting considering the remarkable differences among catalyst structure, operating conditions, and reactor type in the three case studies, which apparently involve different mechanisms of deactivation, including sintering, carbon deposition, and/or attrition and also different reactor configurations.

CONCLUSIONS

Sumptuous synthesis of cobalt catalysts has motivated researchers to develop a more stable catalyst to ensure extended runs of FT industrial units. The cobalt catalyst should be either subjected to repeated regenerations over a reasonable catalyst lifetime or deliver a stable catalytic activity over a long period of time. Developing a realistic

Table 2. Type of Reactor, Reaction Conditions, First co Conversion (X_0), and Run Durations

Case study	Ref.	Catalyst	Reactor type	Run duration	Maximum conversion	Average of conversion	Reaction conditions			
							T (C)	P (bar)	SV ($l/kg_{cat}/h$)	H_2/CO
1	[10]	$Co/\gamma\text{-}Al_2O_3$[a]	Fixed-bed	70 h	63.5782%	47.0742%	220	20	2000	2
1	[10]	$Co/\gamma\text{-}Al_2O_3$[b]	Fixed-bed	70 h	64.3149%	50.7133%	220	20	2000	2
2	[11]	$Pt/Co/P\text{-}Al_2O_3$	CSTR	100 h	85.5596%	51.7984%	230	20	2000	2
2	[11]	$Co/P\text{-}Al_2O_3$	CSTR	100 h	45.4874%	35.716%	230	20	2000	2
3	[12]	$CoPt/Al_2O_3$-A	Capillary cell	500 min	17.9629%	13.1766%	220	20	19600 ($ml\ g^{-1}\ h^{-1}$)	2
3	[12]	$CoPt/Al_2O_3$-N1	Capillary cell	500 min	59.604%	29.8434%	220	20	25000 ($ml\ g^{-1}\ h^{-1}$)	2
4	[13]	$Pt/Co/Al_2O_3$	CSTR	80 h	98.7745%	80.2521%	230	20	2000	2
4	[13]	$Pt/Co/P\text{-}Al_2O_3$	CSTR	80 h	78.1863%	67.9282%	230	20	2000	2
5	[4]	$Co/Pt/Al_2O_3$	slurry bubble column	60 day	70%	60%	220	20	NA	2

[a]Experiment with CO_2 stream. [b]Experiment without CO_2 stream.

Table 3. Average and Standard Deviation for Sigmoid Model Parameters

	a_{SS}	a_L	t_{ip}	k	R-square	Adjusted R-square
Average	0.6052	0.417217	32.185	0.27635	0.991883	0.9907
Standard deviation	0.098441	0.062463	14.13232	0.273304	0.004938	0.005847

model that can perfectly fit the cobalt deactivation rate causes a better fundamental understanding of the deactivation mechanisms and leads to the preparation of more stable catalysts as well as the selection of more appropriate operating conditions. Moreover, such theoretical models facilitate precise control of reactor temperature in petrochemical industry, where the catalyst deactivation decreases the conversion and thus the temperature must be adjusted to maintain the conversion. Accordingly, a modified sigmoid model was introduced to mimic the deactivation rate of cobalt catalyst. Moreover, a comparative discussion was presented based on the

achieved regression parameters.

High values of R-square and adjusted R-square of the fitted models push us to conclude that the introduced novel sigmoid model provides a practical quantification of the catalyst activity for industrial applications. We also may conclude that the introduced model behaves surprisingly more appropriately than GPLEs whether long-term deactivation period or short-term. Furthermore, the sigmoid model can be applicable for a wide range of conditions, including the type of the equipment (fixed bed, CSTR), the feedstock purity, and the test regime. For a future study, sigmoid equation parameters can be considered as a function of catalyst characteristics, operating conditions, and reactants' concentration to achieve a comprehensive model of the catalyst lifetime, which needs extensive investigation in a wide range of operating conditions as well as catalyst structures.

ACKNOWLEDGMENTS

The authors would like to acknowledge the financial supports from the National Petrochemical Company (NPC) of the Islamic Republic of Iran.

REFERENCES

[1] Vik, C. B.; Solsvik, J.; Hillestad, M.; Jakobsen, H. A., Modeling of a slurry bubble column reactor for the Production of biofuels *via* the Fischer-Tropsch synthesis, *Chem. Eng. Technol.* **2015**, *38*, 690-700, DOI: 10.1002/ceat.201400647.

[2] Wood, D. A.; Nwaoha, C.; Towler, B. F., Gas-to-Liquids (GTL): A review of an industry offering several routes for monetizing natural gas, *J. Nat. Gas Sci. Eng.* **2012**, *9*, 196-208, DOI: 10.1016/j.jngse.2012.07.001.

[3] Nakhaei Pour, A.; Taheri, S. A.; Anahid, S.; Hatami, B.; Tavasoli, A., Deactivation studies of Co/CNTs catalyst in Fischer-Tropsch synthesis, *J. Nat. Gas Sci. Eng.* **2014**, *18*, 104-111, DOI: 10.1016/j.jngse.2014.01.019.

[4] Cho, W.; Yu, H.; Ahn, W. -S.; Kim, S. -S., Synthesis gas production process for natural gas conversion over Ni-La_2O_3 catalyst, *J. Ind. Eng. Chem.* **2015**, *28*, 229-235, DOI: 10.1016/j.jiec.2015.02.019.

[5] Bae, J. W.; Kim, S.; Park, S.; Prasad, P. S. S.; Lee, Y.; Jun, K. Deactivation by filamentous carbon formation on Co/aluminum phosphate during Fischer-Tropsch synthesis, *Ind. Eng. Chem. Res.* **2009**, *48*, 3228.

[6] Guo, X.; Lu, Y.; Wu, P.; Zhang, K.; Liu, Q.; Luo, M., The effect of SiO_2 particle size on iron based F-T synthesis catalysts, *Chinese J. Chem. Eng.* **2016**, *24*, 937-943, DOI: 10.1016/j.cjche.2015.12.024.

[7] Fazlollahi, F.; Sarkari, M.; Gharebaghi, H.; Atashi, H.; Zarei, M. M.; Mirzaei, A. A.; Hecker, W. C., Preparation of Fe-Mn/K/Al_2O_3 Fischer-Tropsch catalyst and its catalytic kinetics for the hydrogenation of carbon monoxide, *Chinese J. Chem. Eng.* **2013**, *21*, 507-519, DOI: 10.1016/S1004-9541(13)60503-0.

[8] Atashi, H.; Zohdi-Fasaei, H.; Farshchi Tabrizi, F.; Mirzaei, A. A., Two-level full factorial design for selectivity modeling and studying simultaneous effects of temperature and ethanol concentration in methanol dehydration reaction, *Phys. Chem. Res.* **2017**, *5*, 41-56, DOI: 10.22036/pcr.2017.33491.

[9] Keyvanloo, K.; Fisher, M. J.; Hecker, W. C.; Lancee, R. J.; Jacobs, G.; Bartholomew, C. H., Kinetics of deactivation by carbon of a cobalt Fischer-Tropsch catalyst: Effects of CO and H_2 Partial Pressures, *J. Catal.* **2015**, *327*, 33-47, DOI: 10.1016/j.jcat.2015.01.022.

[10] Kim, S. M.; Bae, J. W.; Lee, Y. J.; Jun, K. W., Effect of CO_2 in the feed stream on the deactivation of Co/γ-Al_2O_3 Fischer-Tropsch catalyst, *Catal. Commun.* **2008**, *9*, 2269-2273, DOI: 10.1016/j.catcom.2008.05.016.

[11] Park, S. -J.; Bae, J. W.; Lee, Y. -J.; Ha, K. -S.; Jun, K. -W.; Karandikar, P., Deactivation behaviors of Pt or Ru promoted Co/P-Al_2O_3 catalysts during slurry-phase Fischer-Tropsch synthesis, *Catal. Commun.* **2011**, *12*, 539-543, DOI: 10.1016/j.catcom.2010.11.008.

[12] Schanke, D.; Hilmen, A. M.; Bergene, E.; Kinnari, K.; Rytter, E.; Ådnanes, E.; Holmen, A., Study of the deactivation mechanism of Al_2O_3-supported cobalt Fischer-Tropsch catalysts, *Catal. Lett.* **1995**, *34*, 269-284, DOI: 10.1007/BF00806876.

[13] Bechara, R.; Balloy, D.; Vanhove, D., Catalytic

properties of Co/Al_2O_3 system for hydrocarbon synthesis, *Appl. Catal. A Gen*. **2001**, *207*, 343-353, DOI: 10.1016/S0926-860X(00)00672-4.

[14] Jacobs, G.; Patterson, P. M.; Zhang, Y.; Das, T.; Li, J.; Davis, B. H., Fischer-Tropsch synthesis: deactivation of noble metal-promoted Co/Al_2O_3 Catalysts, *Appl. Catal. A Gen*. **2002**, *233*, 215.

[15] Li, J.; Zhan, X.; Zhang, Y.; Jacobs, G.; Das, T.; Davis, B. H., Fischer-Tropsch synthesis: Effect of water on the deactivation of Pt promoted Co/Al_2O_3 catalysts, *Appl. Catal. A Gen.* **2002**, *228*, 203-212, DOI: 0.1016/S0926-860X(01)00977-2.

[16] Saib, A. M.; Borgna, A.; Van de Loosdrecht, J.; Van Berge, P. J.; Niemantsverdriet, J. W., XANES study of the susceptibility of nano-sized cobalt crystallites to oxidation during realistic Fischer-Tropsch synthesis, *Appl. Catal. A Gen*. **2006**, *312*, 12-19, DOI: 10.1016/j.apcata.2006.06.009.

[17] Van de Loosdrecht, J.; Balzhinimaev, B.; Dalmon, J. -A.; Niemantsverdriet, J. W.; Tsybulya, S. V; Saib, A. M.; Van Berge, P. J.; Visagie, J. L., Cobalt Fischer-tropsch synthesis: Deactivation by oxidation?, *Catal. Today* **2007**, *123*, 293-302, DOI: 10.1016/j.cattod.2007.02.032.

[18] Visconti, C. G.; Lietti, L.; Forzatti, P.; Zennaro, R., Fischer-Tropsch synthesis on sulphur poisoned Co/Al_2O_3 catalyst, *Appl. Catal. A Gen.* 2007, **330**, *49*-56, DOI: 10.1016/j.apcata.2007.07.009.

[19] Tavasoli, A.; Abbaslou, R. M. M.; Dalai, A. K., Deactivation behavior of ruthenium promoted Co/γ-Al_2O_3 catalysts in Fischer-Tropsch synthesis, *Appl. Catal. A Gen*. **2008**, *346*, 58-64, DOI: 10.1016/j.apcata.2008.05.001.

[20] Moodley, D. J.; Van de Loosdrecht, J.; Saib, A. M.; Overett, M. J.; Datye, A. K.; Niemantsverdriet, J. W., Carbon deposition as a deactivation mechanism of cobalt-based Fischer-Tropsch synthesis catalysts under realistic conditions, *Appl. Catal. A Gen.* **2009**, *354*, 102-110, DOI: 10.1016/j.apcata.2008.11.015.

[21] Khodakov, A. Y., Fischer-Tropsch synthesis: relations between structure of cobalt catalysts and their catalytic performance, *Catal. Today* **2009**, *144*, 251-257, DOI: 10.1016/j.cattod.2008.10.036.

[22] Pansare, S. S.; Allison, J. D., An investigation of the effect of ultra-low concentrations of sulfur on a Co/γ-Al_2O_3 Fischer-Tropsch synthesis catalyst, *Appl. Catal. A Gen.* **2010**, *387*, 224-230, DOI: 10.1016/j.apcata.2010.08.031.

[23] Tan, K. F.; Xu, J.; Chang, J.; Borgna, A.; Saeys, M., Carbon deposition on Co catalysts during Fischer-Tropsch synthesis: A computational and experimental study, *J. Catal.* **2010**, *274*, 121-129, DOI: 10.1016/j.jcat.2010.06.008.

[24] Visconti, C. G.; Lietti, L.; Tronconi, E.; Forzatti, P.; Zennaro, R.; Rossini, S., Detailed kinetics of the Fischer-Tropsch synthesis over Co-based catalysts containing sulphur, *Catal. Today* **2010**, *154*, 202-209, DOI: 10.1016/j.cattod.2010.04.007.

[25] Karaca, H.; Safonova, O. V; Chambrey, S.; Fongarland, P.; Roussel, P.; Griboval-Constant, A.; Lacroix, M.; Khodakov, A. Y., Structure and catalytic performance of Pt-promoted alumina-supported cobalt catalysts under realistic conditions of Fischer-Tropsch synthesis, *J. Catal.* **2011**, *277*, 14-26, DOI: 10.1016/j.jcat.2010.10.007.

[26] Moodley, D. J.; Saib, A. M.; van de Loosdrecht, J.; Welker-Nieuwoudt, C. A.; Sigwebela, B. H.; Niemantsverdriet, J. W., The impact of cobalt aluminate formation on the deactivation of cobalt-based Fischer-Tropsch synthesis catalysts, *Catal. Today* **2011**, *171*, 192-200, DOI: 10.1016/j.cattod.2011.03.078.

[27] Park, S. -J.; Bae, J. W.; Jung, G. -I.; Ha, K. -S.; Jun, K. -W.; Lee, Y. -J.; Park, H. -G., Crucial factors for catalyst aggregation and deactivation on Co/Al_2O_3 in a slurry-phase Fischer-Tropsch synthesis, *Appl. Catal. A, Gen*. **2012**, *413-414*, 310-321, DOI: 10.1016/j.apcata.2011.11.022.

[28] Liu, C.; Li, J.; Zhang, Y.; Chen, S.; Zhu, J.; Liew, K., Fischer-Tropsch synthesis over cobalt catalysts supported on nanostructured alumina with various morphologies, *J. Mol. Catal. A Chem.* **2012**, *363*, 335-342, DOI: 10.1016/j.molcata.2012.07.009.

[29] Sadeqzadeh, M.; Chambrey, S.; Piché, S.; Fongarland, P.; Luck, F.; Curulla-Ferré, D.; Schweich, D.; Bousquet, J.; Khodakov, A. Y., Deactivation of a Co/Al_2O_3 Fischer-Tropsch catalyst by water-induced sintering in slurry reactor: Modeling and experimental

investigations, *Catal. Today* **2013**, *215*, 52-59, DOI: 10.1016/j.cattod.2013.03.022.

[30] Balakrishnan, N.; Joseph, B.; Bhethanabotla, V. R., Effect of Pt and Ru promoters on deactivation of Co catalysts by C deposition during Fischer-Tropsch synthesis: A DFT study, *Appl. Catal. A Gen.* **2013**, *462-463*, 107-115, DOI: 10.1016/ j.apcata.2013.05.001.

[31] Peña, D.; Griboval-Constant, A.; Lecocq, V.; Diehl, F.; Khodakov, A. Y., Influence of operating conditions in a continuously stirred tank reactor on the formation of carbon species on alumina supported cobalt Fischer-Tropsch catalysts, *Catal. Today* **2013**, *215*, 43-51, DOI: 10.1016/j.cattod.2013.06.014.

[32] Tsakoumis, N. E.; Voronov, A.; Rønning, M.; van Beek, W.; Borg, Ø.; Rytter, E.; Holmen, A., Fischer-Tropsch synthesis: An XAS/XRPD combined *in Situ* study from catalyst activation to deactivation, *J. Catal.* **2012**, *291*, 138-148, DOI: 10.1016/ j.jcat.2012.04.018.

[33] Rytter, E.; Holmen, A., Deactivation and Regeneration of commercial type Fischer-Tropsch Co-catalysts-A mini-review. *Catalysts* **2015**, *5*, 478-499, DOI: 10.3390/catal5020478.

[34] Tsakoumis, N. E.; Rønning, M.; Borg, Ø.; Rytter, E.; Holmen, A., Deactivation of cobalt based Fischer-Tropsch catalysts: *A Revi., Catal. Today* **2010**, *154*, 162-182, DOI: 10.1016/j.cattod.2010.02.077.

[35] Saib, A. M.; Moodley, D. J.; Ciobîcă, I. M.; Hauman, M. M.; Sigwebela, B. H.; Weststrate, C. J.; Niemantsverdriet, J. W.; Van de Loosdrecht, J., Fundamental understanding of deactivation and regeneration of cobalt Fischer-Tropsch synthesis catalysts, *Catal. Today* **2010**, *154*, 271-282, DOI: 10.1016/j.cattod.2010.02.008.

[36] Bartholomew, C. H., Mechanism of catalyst deactivation, *Appl. Catal. A Gen.* **2001**, *212*, 17-60, DOI: 10.1016/S0926-860X(00)00843-7.

[37] Tavasoli, A.; Karimi, S.; Taghavi, S.; Zolfaghari, Z.; Amirfirouzkouhi, H., Comparing the deactivation behaviour of Co/CNT and Co/γ-Al_2O_3 nano catalysts in Fischer-Tropsch synthesis, *J. Nat. Gas Chem.* **2012**, *21*, 605-613, DOI: 10.1016/S1003-9953(11)60409-X.

[38] Argyle, M. D.; Frost, T. S.; Bartholomew, C. H., Cobalt Fischer-Tropsch catalyst deactivation modeled using generalized power law expressions, *Top. Catal.* **2014**, *57*, 415-429, DOI: 10.1007/s11244-013-0197-9.

[39] Fuentes, G. A., Catalyst deactivation and steady-state activity: A generalized power-law equation model, *Appl. Catal.* **1985**, *15*, 33-40, DOI: 0.1016/S0166-9834(00)81484-0.

[40] Bartholomew, C. H., Sintering kinetics of supported metals: New perspectives from a unifying GPLE treatment, *Appl. Catal. A Gen*. **1993**, *107*, 1-57, DOI: 10.1016/0926-860X(93)85114-5.

[41] Levenspiel, O., Chemical Reaction Engineering. 3rd ed., John Wiley & Sons, 1999, p. 53.

[42] Mohandas, J. C.; Gnanamani, M. K.; Jacobs, G.; Ma, W.; Ji, Y.; Khalid, S.; Davis, B. H., Fischer-Tropsch synthesis: Characterization and reaction testing of cobalt carbide, *ACS Catal.* **2011**, *1*, 1581-1588, DOI: 10.1021/cs200236q.

[43] Ducreux, O.; Rebours, B.; Lynch, J.; Roy-Auberger, M.; Bazin, D., Microstructure of supported cobalt Fischer-Tropsch catalysts, *Oil Gas Sci. Technol.* **2009**, *64*, 49-62, DOI: 10.2516/ogst:2008039.